# Real-Time Detection of Apnea via Signal Processing of Time-Series Properties of RFID-Based Smart Garments

William M. Mongan*, Ilhaan Rasheed†, Khyati Ved†, Ariana Levitt†, Endla Anday‡, Kapil Dandekar†, Genevieve Dion§, Timothy Kurzweg† and Adam Fontecchio†
*College of Computing and Informatics, †College of Engineering, ‡Department of Pediatrics and §Westphal College of Media Arts and Design: Drexel University, Philadelphia, PA USA

***Abstract*—Signal processing of time-series properties of Radio Frequency Identification (RFID) tags and novel work in textile knitted antennas for garment devices have enabled real-time detection of motion-based artifacts through unobtrusive, wireless, wearable devices. Capturing the Received Signal Strength Indicator (RSSI) as a time-series signal, we classify whether the subject is breathing or not, estimate the rate at which the subject is breathing, and classify whether the tag is moving in a linear, non-stretched fashion. We improve upon previous efforts to classify subject state from RSSI signals by eliminating the need to train the classifier with both breathing and non-breathing sample data (which is biologically infeasible). To test our approach, we use a programmable breathing infant mannequin yielding accurate detection of cessation of respiratory activity within 5 seconds, and a maximum root-mean-square error of 7 per minute when computing the respiratory rate.**

## I. Introduction

Sleep Apnea Syndrome is defined as a reduction of respiratory motion by 95% over a period of 10 seconds, and is a more severe form of hypopnea in which respiration movements decrease below half of their normal values [1]. Many patients who suffer from a sleep disorder such as sleep apnea are unlikely to consult with their physician [2] and may be unaware of their disorder, motivating a mobile continuous monitoring approach; sleep apnea has been associated with an increased risk of heart disease [3].

Our inter-disciplinary team of researchers has developed a smart-fabric wearable device called the "Bellyband" that utilizes conductive thread and an Radio Frequency Identification (RFID) tag to wirelessly monitor motion-based state of a subject, such as respiratory activity [4]. As the subject breathes, the chest-wall and abdomen stretch outward, causing the conductive yarns of the garment to elongate and retract. A remote RFID interrogator continuously and wirelessly polls the Received Signal Strength Indicator (RSSI) of the RFID tag, yielding a time-series signal that is monitored to detect changes in subject state, respiratory rate, and other properties. Because the RFID tag is passive, the chip is energized by the wireless RFID interrogation signal and no battery or wire is required to power the chip on the garment device. As shown in Figure 1, the RSSI changes in an oscillatory pattern during respiration activity, and in a possibly-oscillatory pattern during other motion activities.

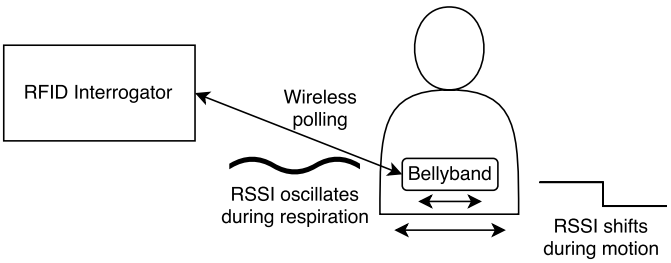


Fig. 1: RSSI data fluctuates in a sinusoidal pattern during respiratory motion as the Bellyband elongates and retracts during chest wall motion, while non-oscillatory motion affects the RSSI in a non-oscillatory pattern during movement of the entire Bellyband relative to the interrogator.

The passive, powerless RFID signal presents uncertainty that is exacerbated by any non-respiratory "ambient" motion introduced by the subject. As a result, statistical modelling is required to make probabilistic inference about the state of the subject. This is necessary because the primary measure from the Bellyband under consideration, the RSSI, is not linearly separable between breathing and non-breathing states on its own because of the noise artifacts observed in the data. Additionally, the machine learning algorithms require large quantities of training samples to classify whether or not the subject is breathing, and it is infeasible to collect data while the subject is known to be in an anomalous state such as non-breathing (especially if the subject is an infant).

In this paper, we apply filtering, signal processing, statistical analysis, and machine learning approaches to detect cessation of respiration within 5 seconds, estimate respiration rate and a change in respiration rate to half its normal value within 10 seconds, and determine when non-respiratory motion of the subject (which may interfere with these respiratory state classifications) has taken place.

The rest of this paper is organized as follows: in Sections II and III we describe the related efforts to and background of our problem; our approach is detailed in Section IV, including the conductive knit-antenna and fabric design (Section IV-A),

respiration cessation detection (Section IV-B), respiratory rate estimation (Section IV-C), and ambient motion detection (Section IV-D). Our results are summarized in Section V, and we conclude in Section VI.

## II. Related Work

With the advent of wearable technology, there has been great interest in smart textiles that can enable real-time, continuous monitoring. Such technology has the potential to open up new avenues for improved healthcare and wellness. They provide the possibility to continuously monitor vital signs, allowing medical practitioners to administer preventative treatments to patients who may be at risk of serious illness. Other potential application areas for smart textile devices also include enhancing first responder safety [5].

Textile antenna based technology face several impediments from mass market penetration. First, the physical flexibility of textile antennas pose reliability issues for wireless communication protocols. Second, the lack of mass production techniques have made them cost prohibitive for commercialization [6]. Most smart textile systems rely on the integration of powered transceivers with conventional fabric to attain smart functionality. This results in devices that are bulky, uncomfortable and power hungry. These drawbacks make contemporary garment systems unreliable for long term patient monitoring.

A passive RFID based sleep monitoring system called NightCare has been described in [7]. This system uses flexible tags integrated in clothing and conventional tags placed on beds and surrounding areas. A real-time software engine uses readings from these tags to determine motion, accidental falls, long-term absence and interaction with nearby objects. An alarm is generated in the event of an emergency such as a fall. The software can also generate reports and statistics on sleep positions which can be used in the diagnosis of sleep related disorders such as apnea and bedsores, but does not provide real-time respiration or heart rate information.

Alternative wireless health monitoring systems have been proposed that alleviate the need for any device to be placed on the human body. One such system is Vital-Radio, which uses wireless signals to monitor respiration and heartbeats [8]. Vital-Radio transmits a low-power wireless signal and measures the time it takes to reflect back to the device. Respiration and heartbeats cause variations in the reflection time, which is used by the system to extract rates. While this system enables convenient vital sign monitoring in a home environment, it is not practical for hospital use since it cannot guarantee privacy for all individuals within wireless range of the system and requires 1.5 meter separation between patients.

Our current smart textile system uses passive UHF RFID chips integrated into textile antennas composed of conductive and non-conductive fabrics. The RFID chip is inductively coupled with a co-planar micro-strip fabric antenna and is placed in a small knitted pocket in the center of the antenna. Passive UHF RFID does not require a dedicated power source and can be powered by an interrogating UHF RFID reader. Deformation of our textile antenna, known as Bellyband, results in a variation of it's backscatter power (RSSI) [9]. This variation in RSSI is detected by the RFID reader and can be used to infer actuation of the Bellyband.

## III. Background

Apnea is defined as a cessation in respiratory activity for a period of 10 seconds or more. In this effort, we aim to detect a reduction in respiratory movement and rate more quickly, so that the result can be generalized to Sleep Apnea Syndrome symptom detection and other non-respiratory motion-based monitoring applications. Therefore, we consider time-series properties of RFID interrogations such as RSSI over short time periods called "windows", *i.e.*, 0.2 to 1.0 second per window, to facilitate real-time signal processing.

To interrogate the RFID-based Bellyband, an Impinj Speedway R420 RFID interrogator is used. The Impinj Speedway communicates using the Low Level Reader Protocol (LLRP) over a TCP/IP network connection. Utilizing an RFID tag RSSI value as a time-series signal that can be correlated to respiratory depth, frequency, and rate, is a challenge because the RFID interrogator must "channel hop" between 50 frequencies ("channels") within the 902-928MHz (UHF) band utilized by RFID applications in the United States. The interrogator must spend no more than 0.4 seconds in a 20-second period interrogating on any one frequency per Federal Communications Commission (FCC) regulations [10].

The backscatter power received by a RFID reader from a tag can be mathematically modeled by Equation 1 [11].

$$P_{Rx,reader} = P_{Tx,reader} G_{reader}^2 G_{tag}^2 \Big( \frac{\lambda}{4 \times \pi \times r} \Big)^4 R \quad (1)$$

where $P_{Rx,reader}$ is the backscatter power received by the reader, $P_{Tx,reader}$ is the reader transmit power (30 dBm), $G_{tag}$ and $G_{reader}$ are the RFID tag and reader gain, respectively, $\lambda$ is the wavelength of the interrogation wave, $r$ is the distance between the reader and tag, and $R$ is the backscatter transmission loss.

It is evident from the equation that variation in $\lambda$ (due to channel hopping) can cause minor fluctuations in $P_{Rx,reader}$, which can then affect RSSI readings. This, along with variations in antenna properties due to physical deformation, result in frequent changes to the measured RSSI. This can be seen in Figure 2 as the square-waves of approximate magnitude 1 dBm modulating the RSSI time-series plot, varying every 200 milliseconds. In order to filter out noise artifacts from the signal, and to capture a significant portion of respiratory motion in the signal, a window greater than 200 milliseconds is needed for processing; therefore, it is necessary to consider signals spanning multiple frequency channels in the same signal processing algorithm, even though the change in interrogation frequency changes the signal as a noise artifact. To account for this, the RSSI signals observed during a period in which the RFID interrogator is focused on a single frequency are separated by the RFID tag observed and called a "channel burst". Then, each RSSI data point $x$ is replaced with $x - \bar{x}$, where $\bar{x}$ is the mean RSSI of the channel burst containing data point $x$, normalizing the RSSI by the "channel burst mean."

We collect the RSSI as well as other properties from the RFID interrogator, including the Doppler shift, phase, and RFID frequency. These properties are useful for detecting "ambient" motion of the RFID tag, that is, motion unrelated to the stretching behavior of the textile being monitored. According to the Impinj documentation [12], the Doppler shift is observed over a single tag, rather than as a phase difference between two tags, in order to avoid inconsistencies due to channel hopping. The use of a single tag sacrifices frequency estimation accuracy [13]; we utilize two successive RFID interrogations using the same channel, antenna, and RFID tag and compute the tag velocity from the phase difference according to Equation 2 [13]:

$$v = \frac{c * (\phi_2 - \phi_1)}{f * (t_2 - t_1)} \tag{2}$$

where $c$ is the speed of light in a vacuum, $\phi$ is the measured phase of a tag interrogation, $t$ is the time of that interrogation, and $f$ is the frequency in the 900MHz band that the interrogator used to make that interrogation.

## IV. Approach

### A. Antenna Manufacturing: Knit Structure and Yarn Selection

The bellyband is knitted on an SSG-122SV Shima Seiki knitting machine using Shima Seiki's SDS-ONE APEX3 proprietary design system. The antenna is knit with conductive and nonconductive threads. The antenna arms are knitted with silver-coated nylon yarn and the nonconductive slot is knitted with blends of viscose and polyamide. A thin Printed Circuit Board (PCB) with a soldered RFID chip is inserted into the pocket during the knitting process. During stretching of the antenna, we faced coupling issues between the RFID chip and the textile antenna arms. To improve the inductive connection between the antenna and the chip, we knitted the conductive yarns into the pocket using tuck stitches, stitches elongated in the wale (lengthwise) direction.

### B. Respiration Cessation Classification

Detection of the cessation of respiration activity is an important application of the Bellyband sensor. Signals from the sensor need to be classified as breathing or non-breathing in real time in order to make the Bellyband a reliable biomedical monitoring device. Here, we design a classifier using statistical analysis of features of RSSI time-series data to detect cessation of respiration using the Bellyband.

*1) Machine Learning Classification:* In our previous work [14], a Support Vector Machine (SVM) was constructed around training data and then applied to subsequent samples to determine the respiratory state of the subject. This introduced some challenges: first, it was biologically infeasible to train the classifier on both breathing and non-breathing data, since non-breathing training samples would require an infant to voluntarily stop breathing activity; second, to attain an error rate upper-bound of 0.01% with 95% confidence requires 5 hours of interrogation samples [15] [16] [17]. A One-Class SVM exists to classify novelty data trained only against "normal" (*i.e.*, breathing) class data points, but this classifier works by forming a boundary around the training data and classifying novelty data as any such points that fall outside of that bound. For respiratory analysis, a One-Class SVM classifies "unusually" deep breathing as novelty data as well as a cessation of respiration.

Using the Bellyband sensor, the cessation of breathing can be detected by using an SVM. Signals collected from the Bellyband can be provided to an SVM whose training class is determined *a priori*. Chest wall motion due to respiration will result in actuation of the Bellyband sensor. Therefore, the cessation of breathing can be determined by detecting non-actuation. Actuation and non-actuation can be two classes that can be classified by a SVM. However, this would require a SVM to be trained on non-actuation, thereby requiring a patient to cease respiration for part of the training period. This is not viable for infant applications, and requires a novel approach to training set generation or a One-Class Support Vector Machine. These approaches have yielded classification accuracy between 70% and 94% in prior efforts.

*2) Statistical Testing for Classification:* If a classifier is used that avoids requiring large quantities of training samples, and single-class anomaly detection machine learning algorithms, we can attain more predictable and consistent classification accuracy results. The Short-Time Fourier Transform (STFT) yields magnitudes representing change in amplitude of the RSSI signal over various frequencies for each of the short-time windows in use. This multi-dimensional array of FFT magnitudes is known as the spectrogram of the signal. We compute the mean of the power spectral density magnitudes to determine the average amplitude deviation per unit of frequency of the signal as a sample data point. The first $N$ samples are reserved as training data, and a t-test [18] (Equation 3) is applied to subsequent samples to determine the likelihood that they were drawn from the same distribution as the training samples.

$$t = \frac{s - \mu}{\sqrt{\frac{\sigma^2}{n}}} \tag{3}$$

where $s$ is the sample (the mean RSSI over the past $T_s$ second window), $\mu$ and $\sigma^2$ are the mean and variance, respectively, of all samples collected during the training period, and $n$ is the number of training samples collected.

If we are less than 95% confident ($p < 0.05$) that the sample is drawn from the same distribution as the training samples, the null hypothesis that the sample *is* drawn from the same distribution is rejected. As with the One-Class SVM, this could mean that the subject is no longer breathing, or that the subject is breathing more deeply than during training. If the mean of the sample is less than the mean of the training samples, we conclude that the null hypothesis was rejected because the subject is experiencing more shallow breathing than during training, or no respiratory activity at all.

### C. Respiration Rate Estimation

While detecting the cessation of respiration can alert patients to potentially dangerous conditions, respiration rate can be used for analysis of respiration patterns over time. Changes in respiration can be used to detect potential respiratory illnesses, such as Sleep Apnea Syndrome, and appropriate treatments can be administered in a timely manner.

Estimating the rate of oscillation of the time-series signal is a challenge because a finer estimate of the state is required than for binary state classification (*i.e.*, breathing or non-breathing) at a given point in time. However, for respiration rates up to $60 * T_s^{-1}$ per minute, where $T_s$ is the window period used in state classification (*i.e.*, 0.5 seconds), we can use the classification obtained in Section IV-B to inform respiration rate. If we determine that respiration was the detected class for $N$ out of the past $M$ windows of size $T_s$ seconds, then the respiration rate is $60 * \frac{1}{2} * \frac{N}{M*T_s}$. The additional factor of $\frac{1}{2}$ is used because detection of respiratory motion in a particular window is a detection of the motion required to inhale or exhale; that is, the $N$ observed actuating windows accounts for twice the number of full respirations. These averages are then estimated using a Kalman filter [19] and averaged over the past $k$ seconds to provide a smooth estimator of respiration rate. A Kalman filter is used because there is some uncertainty inherent in the sensor measurements due to the wireless medium and the known RSSI variance of 1 provided by the Impinj RFID interrogator being used. The subsequent averaging of instantaneous rates is to account for the inaccuracy that results from extrapolating a rate over a 1 minute period by taking only a few seconds' worth of samples. For smoothing, we inspect such samples over a longer period of time and gradually update the estimate with new data via long-term averaging (using a 6-second window).

### D. Real-Time Motion Detection

We used the spectral power spectrogram resulting from the STFT described in Section IV-B over windows of RSSI signals to classify respiratory activity and rate. Since the STFT is used to determine periodic oscillations in the data, such as that exhibited by the inhale-exhale motion of respiration, the spectrogram is not applicable to detecting ambient (*i.e.*, non-respiratory) motion as the RSSI reduces when the subject moves backwards and increases when the subject moves in the forward direction. Oscillation is not assured in non-respiratory motion; accordingly, the Fisher Discriminant Ratio (FDR) indicated low separability of spectral power. Instead, we observe the change in channel-normalized RSSI over time by computing its slope over small time windows. As the subject moves away from the antenna, the received power reduces and thus, the value of RSSI decreases. RSSI is correlated to "backward" or "forward" motion.

For motion classification, we first use the method of local regression to smoothen the RSSI data: specifically, Locally-Weighted Scatter Plot Smoother (LOESS). The smoothing process is considered local because each smoothed value is determined by neighboring data points defined within the span. Here, local regression is used to filter out respiratory oscillations from less-fine ambient movements. Using the span, a regression weight function is defined for the data points withing that span via Equation 4:

$$w_i = \left(1 - \left|\frac{x - x_i}{d(x)}\right|^3\right)^3 \tag{4}$$

Here, $x$ is the predictor value associated with the response value to be smoothed, $x_i$ are the nearest neighbors of $x$ as defined by the span, and $d(x)$ is the distance along the abscissa from $x$ to the most distant predictor value within the span. In our case, we used the span of 50% so as to flatten out the oscillations in normalized RSSI due to breathing.

To compute the slope of change in RSSI, we consider windows of length two seconds up to time $N$ over the intervals $[k, k+2], \forall k \in [0, N-2)$. For each window, we consider the first and the last value of RSSI and calculate its slope using the equation of slope of the line over time: $slope = \frac{\Delta RSSI}{\Delta t}$.

As we are smoothing the data using the method of local regression, as described above, if we inhale to an exhale in the next window the data is flat so we do not get a sudden changes in slope, as shown in Figure 2.

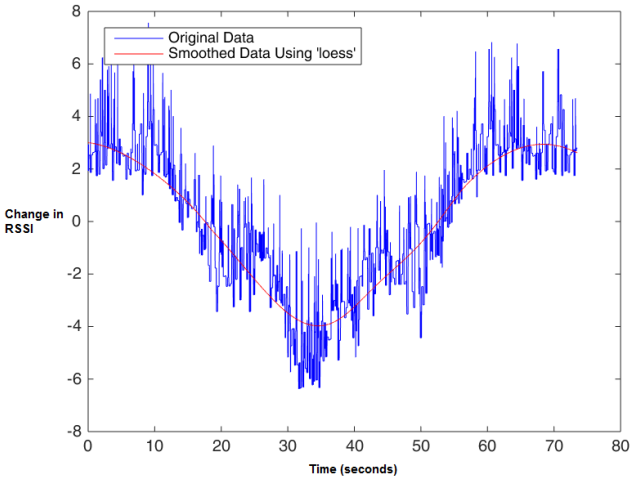


Fig. 2: Using local regression, the time-series data is smoothed over small windows by performing regression weighting against near-neighbors of the data, filtering the backwards and forwards motion of the mannequin from the oscillatory pattern exhibited by respiratory motion.

In case of sudden movements, due to smoothing more points are classified as a movement thus, another method was developed to separately detect a sudden movement. This method calculates the average of normalized RSSI data over each of the two seconds windows. Then, each of those averages are compared with the average of the previous window. If it remains within the threshold we consider the movement to be of a continuous form otherwise, we flag it as a sudden movement in that particular window.

## V. Results

### A. Cessation Classification

In our experiment, a Laerdal SimBaby programmable infant mannequin [20] was programmed to breathe at a rate of 31 per minute for 1 minute, then stop breathing for 1 minute, alternating between these states for a period of time. Subsequently, the mannequin was programmed to breathe at a rate of 31 per minute for 1 minute, then at a rate of 15 per minute for 1 minute, then stop breathing for one minute, then at a rate of 15 for 1 minute, and finally at a rate of 31 again for 1 minute. The interrogator was positioned approximately 1-3 feet from the mannequin, oriented above, astride, or at the feet. The STFT considered non-overlapping windows of 0.5 seconds in size and a training window period of 20 seconds, yielding a sample population size of 40 for the t-test.

Lack of respiratory activity is not necessarily sleep apnea; recall that apnea is defined as a cessation in respiratory motion for a period of 10 seconds or more. Moreover, a detected cessation in respiratory activity by a Short-Time Fourier Transform merely indicates that no respiratory activity occurred during that short-time window. This could be caused by the natural pause that occurs between respirations or between inhale and exhale. In order to better generalize our approach to other biomedical detection applications, we measured a cessation of respiration as cessation detected by our approach for $M$ consecutive short-time windows, where $M$ is defined to be greater than the number of short-time windows within the maximum respiratory period programmed to the SimBaby. In this experiment, the minimum rate was 15 respirations per minute, or a maximum period of 4 seconds between respirations. Since the STFT short-time window $T_s$ was chosen to be 0.5 seconds, and the maximum period $T_{max}$ is 4 seconds, $M = \frac{T_{max}}{T_s} = 8$ consecutive window periods was chosen. Cessation was detected within 4 seconds when oscillating between a respiratory rate of 31 and 0, and within 5 seconds when oscillating between a respiratory rate of 31 to 15 to 0, with no false positives or false negatives in either case.

### B. Rate Detection

Because we are able to classify respiratory state (*i.e.*, breathing or non-breathing) using short time windows ($T_s = 0.5$), these results are suitable for estimating respiratory rate by observing when the subject was observed to be stretching the band either during a particular inhale or exhale motion, and interpolating over a one-minute period to obtain the rate. Using the same experimental data collected in Section IV-B, we estimated the rate during breathing periods to be 33 and 28 respirations per minute after eliminating the 6-second transition period between breathing periods, when the SimBaby was programmed to breathe at 31 per minute, as shown in Figure 3a, and estimated breathing rates of 38, 18, 18, and 31 respirations per minute for the breathing periods shown in Figure 3b, when the ground truths from the SimBaby were set at 31, 15, 15, and 31, respectively. These results correspond to root-mean-squared errors of 4 and 7 per minute, respectively (the errors are 9 and 8, respectively, if the 6-second transition period is used in the error calculation).

### C. Ambient Motion

In this experiment, we collected 10 seconds of data with the band moving away from the antenna, followed by 10 seconds in which the band moves towards the antenna. The slopes are calculated and utilized along with the doppler frequency and the velocity by phase difference (Equation 2) to train a neural network for classification. To measure the separability of statistical features such as the RSSI, doppler and velocity between the "forward" and "backward" motion classes, the FDR was applied to several statistical features of the windows, and predicted the RSSI, doppler and velocity to be separable and therefore good candidates for our classification analysis.

We obtained ≈86% motion classification accuracy using Neural network for classification and 95%-98% using the slope and threshold approach. For sudden movements, using the average method, we had 100% accuracy in detecting the instant at which the movement had occurred.

## VI. Conclusion and Future Work

In this paper, we normalized RFID signal strength (RSSI) data by frequency and calculated the tag velocity in order to utilize the signal for respiratory analysis. The resulting time-series data was filtered and signal processed to determine the mean power spectral density, derived from the amplitude of the oscillatory behavior observed in the signal during short time windows. This was correlated to respiratory activity by applying a t-test to compare the power spectral density to those collected during a brief training period in which the subject was breathing normally. This yielded highly accurate classification results, and the short time windows of the STFT were conducive to utilizing respiratory classification results to estimate the respiratory rate as well. These results were collected well within the time period to needed to detect apnea and hypopnea. Finally, we used the RSSI slope over time to observe "ambient" motion artifacts.

As future work, we plan to expand on the respiratory classifier to detect respiratory depth, *i.e.*, a change from normal to shallow respiratory activity. Additionally, we will study the respiration rate estimator in more detail by using a sliding window classifier that could detect changes in respiratory state with finer granularity in time, rather than during discretized time windows. We will study the generalization of our ambient motion detection approach to rotational and lateral motion artifacts, and we will use data fusion to utilize these classification sensors to inform one another in real-time to reduce classification and estimation uncertainty. Finally, we will use readings obtained from the Bellyband to compute antenna characteristics such as gain and return loss over a frequency range in order to develop an accurate mathematical model for the observed RSSI fluctuations.

## Acknowledgment

Our research results are based upon work supported by the National Science Foundation Partnerships for Innovation:

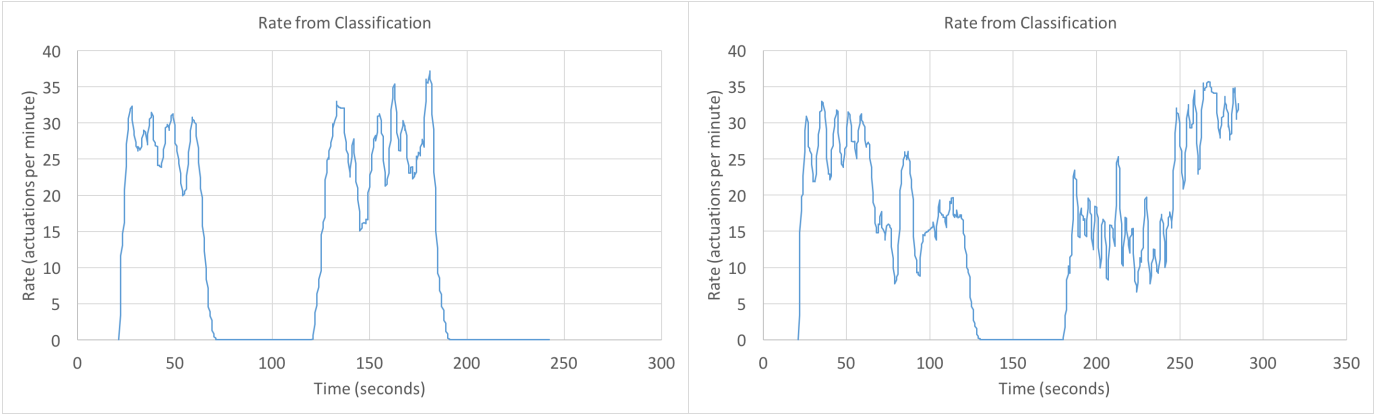


(a) Stretching at 31, 0, 31, 0 per minute for 1 minute each

(b) Stretching at 31, 15, 0, 15, 31 per minute for 1 minute each

Fig. 3: Rate estimation over time for two experimental runs, computed as the number of actuation classifications made in the past $k = 6$ seconds extrapolated to a one-minute rate. Note that the plots begin after 20 seconds because the first 20 seconds of data are reserved for training the classifier used in computing the rates.

Building Innovation Capacity (PFI:BIC) subprogram under Grant No. 1430212. Any opinions, findings, and conclusions or recommendations expressed in this material are those of the author(s) and do not necessarily reflect the views of the National Science Foundation. Research reported in this publication was supported by National Institute of Biomedical Imaging and Bioengineering of the National Institutes of Health under award number U01EB023035. The content is solely the responsibility of the authors and does not necessarily represent the official views of the National Institutes of Health.

## REFERENCES

[1] R. Begg and M. Palaniswami, *Computational Intelligence for Movement Sciences: Neural Networks and other Emerging Technologies*. Idea Group Publishing, 2006.

[2] D. Mack, M. Alwan, B. Turner, P. Suratt, and R. Felder, "A Passive and Portable System for Monitoring Heart Rate and Detecting Sleep Apnea and Arousals: Preliminary Validation," in *Distributed Diagnosis and Home Healthcare, 2006. D2H2. 1st Transdisciplinary Conference on*, April 2006, pp. 51–54.

[3] D. J. Gottlieb, G. Yenokyan, A. B. Newman, G. T. O'Connor, N. M. Punjabi, S. F. Quan, S. Redline, H. E. Resnick, E. K. Tong, M. Diener-West, and E. Shahar, "Prospective Study of Obstructive Sleep Apnea and Incident Coronary Heart Disease and Heart Failure," *Circulation*, vol. 122, no. 4, pp. 352–360, 2010. [Online]. Available: http://circ.ahajournals.org/content/122/4/352

[4] W. Mongan, E. Anday, G. Dion, A. Fontecchio, K. Joyce, T. Kurzweg, Y. Liu, O. Montgomery, I. Rasheed, C. Sahin, S. Vora, and K. Dandekar, "A Multi-Disciplinary Framework for Continuous Biomedical Monitoring Using Low-Power Passive RFID-Based Wireless Wearable Sensors," in *2016 IEEE International Conference on Smart Computing (SMARTCOMP)*. IEEE, 2016, pp. 1–6.

[5] T. Gao, C. Pesto, L. Selavo, Y. Chen, J. Ko, J. Lim, A. Terzis, A. Watt, J. Jeng, B. R. Chen, K. Lorincz, and M. Welsh, "Wireless Medical Sensor Networks in Emergency Response: Implementation and Pilot Results," in *Technologies for Homeland Security, 2008 IEEE Conference on*, May 2008, pp. 187–192.

[6] H. Rogier, "Energy-Efficient Textile Antenna Systems for Body-Centric Communication and Sensing," in *Radio Science Conference (URSI AT-RASC), 2015 1st URSI Atlantic*, May 2015, pp. 1–1.

[7] S. Amendola, R. Lodato, and S. Manzari, "RFID technology for IoT-based personal healthcare in smart spaces," *Internet of Things*, vol. 1, no. 2, pp. 144–152, 2014. [Online]. Available: http://ieeexplore.ieee.org/xpls/abs_all.jsp?arnumber=6780609

[8] F. Adib, H. Mao, Z. Kabelac, D. Katabi, and R. C. Miller, "Smart Homes that Monitor Breathing and Heart Rate," *Proceedings of the 33rd Annual ACM Conference on Human Factors in Computing Systems - CHI '15*, pp. 837–846, 2015. [Online]. Available: http://dl.acm.org/citation.cfm?doid=2702123.2702200

[9] D. Patron, W. Mongan, T. P. Kurzweg, A. Fontecchio, G. Dion, E. K. Anday, and K. R. Dandekar, "On the Use of Knitted Antennas and Inductively Coupled RFID Tags for Wearable Applications," *IEEE Transactions on Biomedical Circuits and Systems*, vol. PP, pp. 1932–4545, 2016. [Online]. Available: http://ieeexplore.ieee.org/lpdocs/epic03/wrapper.htm?arnumber=7458913

[10] U. G. P. Office, "Electronic Code of Federal Regulations, Title 47, Chapter I, Subchapter A, Part 15.247," http://www.ecfr.gov/cgi-bin/text-idx?node=pt47.1.15&rgn=div5#se47.1.15_1247.

[11] Z. Su, S. C. Cheung, and K. T. Chu, "Investigation of radio link budget for UHF RFID systems," *Proceedings of 2010 IEEE International Conference on RFID-Technology and Applications, RFID-TA 2010*, no. June, pp. 164–169, 2010.

[12] Impinj, "Application Note - Low Level User Data Support," https://support.impinj.com/hc/en-us/article_attachments/200774268/SR_AN_IPJ_Speedway_Rev_Low_Level_Data_Support_20130911.pdf.

[13] J. Han, H. Ding, C. Qian, W. Xi, Z. Wang, Z. Jiang, L. Shangguan, and J. Zhao, "CBID: A Customer Behavior Identification System Using Passive Tags," *IEEE/ACM Transactions on Networking*, vol. PP, no. 99, pp. 1–1, 2015.

[14] W. Mongan, K. Dandekar, G. Dion, T. Kurzweg, and A. Fontecchio, "Statistical Analytics of Wearable Passive RFID-based Biomedical Textile Monitors for Real-Time State Classification," in *2015 IEEE Signal Processing in Medicine and Biology Symposium (SPMB)*, Dec 2015, pp. 1–2.

[15] Y. S. Abu-Mostafa, M. Magdon-Ismail, and H.-T. Lin, *Learning From Data*. AMLBook, 2012.

[16] V. Vapnik, E. Levin, and Y. Cun, "Measuring the VC-dimension of a Learning Machine," *Neural Computation*, vol. 6, pp. 851–876, 1994.

[17] D. Hush and B. Horne, "Progress in Supervised Neural Networks," *Signal Processing Magazine, IEEE*, vol. 10, pp. 8 – 39, 1993.

[18] P. L. Witt and P. McGrain, "Comparing Two Sample Means t Tests," *Physical Therapy*, vol. 65, no. 11, pp. 1730–1733, 1985. [Online]. Available: http://ptjournal.apta.org/content/65/11/1730

[19] R. E. Kalman, "A New Approach to Linear Filtering and Prediction Problems," *Transactions of the ASME–Journal of Basic Engineering*, vol. 82, no. Series D, pp. 35–45, 1960.

[20] Laerdal, "Laerdal Simbaby and Linkbox," http://www.laerdal.com/us/item/245-02001, 2001.